

PRODUCTION OF CLIC ACCELERATING STRUCTURES USING DIFFUSION BONDING AT VERY HIGH TEMPERATURE

A. XYDOU¹, M. AICHELER², E. RODRIGUEZ CASTRO³,
N.J. SIAKAVELLAS⁴ & S. DOEBERT⁵

^{1,2,3,5}CERN, European Organization for Nuclear Research

^{1,4}UoP, University of Patras, Nuclear Technology Laboratory

³University of Vigo

²HIP, Helsinki Institute of Physics

ABSTRACT

Diffusion bonding is a process used in the fabrication of the accelerating structures of the Compact Linear Collider (CLIC). The preservation of the required micro-precision tolerances and the quality of the final bonded joint are the main objectives in this paper. Diffusion bonding tests were conducted with OFE Oxygen-Free Electronic Copper (Cu-OFE) disks with simple and radio frequency (rf) geometry, with variable values of applied pressure and interface flatness. Ultrasound and tensile tests were carried out with the bonded samples in order to qualify the bonded joints. The analytical approach used the creep mechanisms of Nabarro-Herring and Coble and the comparison with experimental results of the permanent deformations showed good agreement. The quality of the final bonded joint showed no dependence on the applied pressure or on the flatness of the joint surfaces.

KEYWORDS: CLIC, Diffusion Bonding, Diffusion Creep, High Temperature, Copper OFE

Received: Jan 11, 2016; **Accepted:** Apr 07, 2016; **Published:** Apr 09, 2016; **Paper Id.:** IJMMSEAPR20164

INTRODUCTION

CLIC [1] is a study for a future linear collider for high energy physics which relies on a new two-beam acceleration concept. The CLIC design foresees two meter long two-beam modules and will operate under ultra-high vacuum conditions required for beam transport. The two-beam modules consist of high-gradient accelerating structures to accelerate the main beam and decelerating structures to extract the rf power from the drive beam at 12 GHz. The accelerating structures operate with very high electrical surface fields of the order of almost 300 MV/m. To sustain these high electrical fields and avoid electrical breakdowns the inner rf surface of these structures has to be ultra clean and smooth. Each accelerating structure is build out of ~30 disks which are jointed together by diffusion bonding under very high temperature, close to the melting point of copper and in a hydrogen atmosphere. This process turned out to be the most successful to obtain very clean and smooth surface which allow for these ultra-high electrical fields. In addition to preserve the beam quality in the linear accelerator the geometry of the rf structure has to be very precise to control the higher order modes in these resonators. The shape tolerance for a disk and for the assembly is in the micrometer range.

Diffusion bonding is a solid state process [2], [3] of welding which is capable of joining a wide range of metals and ceramics by the inter diffusion of atoms across their interface. The diffusion bonding is conducted at elevated temperatures typically above 0.6 of the absolute melting point (T_m) of the base material in vacuum, or in a

gas atmosphere in order to reduce the oxidation of the surfaces in contact.

The assembly procedure of the accelerating structures is constituted of several steps involving high precision machining as well as heating cycles at very high temperatures and quality controls. The machining tolerances for the rf shape are in the range of 0.005 to 0.02 mm, for the flatness is 0.001 mm and for the roughness (Ra) is in the range of 0.025 to 0.1 μm and they should be preserved after the heating cycle, in order to fulfill the rf and beam dynamics constraints.

THEORETICAL REVIEW

Diffusion bonding [4], [5] is performed at temperature close to the melting point of the tested material and low applied stresses. Due to these conditions, the diffusional process [6] takes place and leads to creep deformation. This process begins with the sliding of grain boundaries, creating a depletion of vacancies along their length, which experience a compressive stress [7]; while a corresponding excess of vacancies experiences a tensile stress. The material is moving perpendicularly to the direction of the compressive regions to those with tensile stresses. To this end, diffusion creep refers to the stress directed flow of vacancies that take place in order to restore an equilibrium condition. During this process the vacancy flow may occur through the crystalline matrix and is known as Nabarro-Herring diffusion creep or along the grain boundaries with a process known as Coble diffusion creep [8], [9]. The theory developed independently by Nabarro and Herring for lattice diffusion of vacancies from grain boundaries under tension to those under compression, predicts linear variation of strain rate with stress and inverse-squared dependence on grain size.

The tensile creep rate is given by the equation (1):

$$\dot{\epsilon}_{\text{NH}} = A_{\text{NH}} \frac{D_l \Omega \sigma}{d^2 k T} \quad (1)$$

where A_{NH} is a constant having a theoretical value lying within the range approximately 12-40 [10] depending on the shape of the grains, the grain size and the load distributions. Ω is the atomic volume, σ is the applied stress, D_l is the coefficient for lattice self-diffusion, d is the grain size which had been measured and had an average value of 65 μm , k is Boltzmann's constant and T is the absolute temperature.

The creep rate which gives the diffusion creep along the grain boundaries according to Coble is given on the equation (2):

$$\dot{\epsilon}_{\text{Co}} = A_{\text{Co}} \frac{\delta D_{\text{gb}} \Omega \sigma}{d^3 k T} \quad (2)$$

where A_{Co} is approximately $150/\pi$ [10], δ is the effective width of the grain boundary for vacancy diffusion and D_{gb} is the coefficient for grain boundary diffusion. Concluding, Coble's creep mechanism for $T < 0.7 T_m$ (where $T_m = 1356 \text{ K}$ is the melting point of copper) is considered dominant; while for $T > 0.7 T_m$ Nabarro-Herring diffusion creep is considered dominant [11].

EXPERIMENTAL PROCEDURE

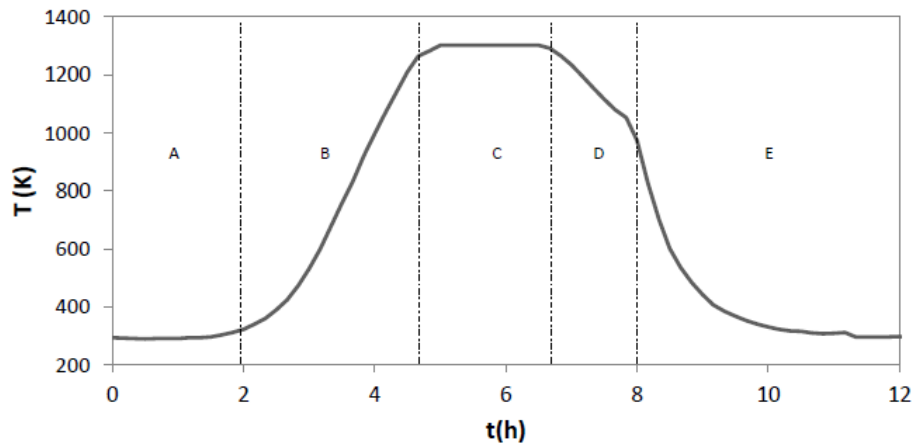


Figure 1: Heating Cycle: A) Vacuum is pumped to the Furnace, B) When the vacuum level is at 10^{-5} mbar the H_2 is injected and the furnace is heated Up ($5^\circ\text{C}/\text{min}$), C) The temperature stays at 1298 K for 150 Minutes, D) First controlled cooling down to 800 K for 60 min under Ar, E) Fast cooling down to the room temperature for approximately 250 min under Ar.

In this experimental program two different studies were conducted. The first study investigated the effect of the applied pressure on the final deformations and the quality of the final bonded joint. The second study examined the dependence of the flatness in the interface of the disks on the quality of the final bonded joint.

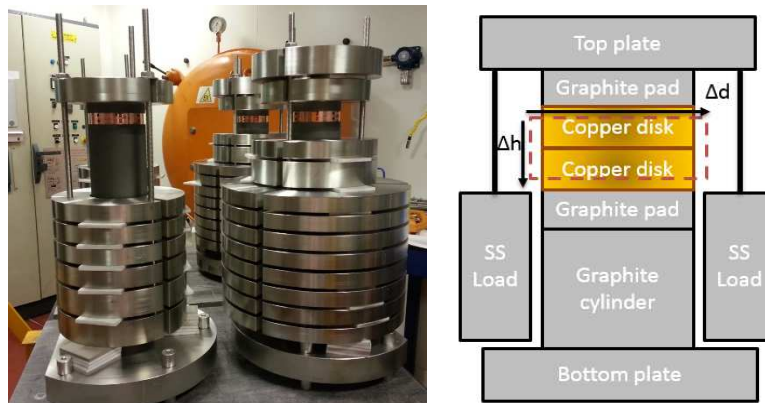
The work flow that was followed was common in both studies before the bonding process. Grain size analysis was performed in two disks of each group so as to have an indication of an average grain size at room temperature. Next step was the cleaning of the disks [12], in order to remove as much as possible of the oxide layer on their surfaces. Afterwards, the dimensional control had taken place where the dimensions of the disks were measured with an ultra high precision coordinate measuring machine (CMM) [13]. The heating cycle that was followed in all the cases during the diffusion bonding is presented in Figure 1. The high temperatures together with the H_2 environment are required for the structures high-gradient performance [14].

Each configuration (Figure 2(a)) inside the furnace consisted of two disks and two graphite pads below and above like a sandwich material. The loads were from stainless steel and they were transferring their weight to the copper disks through three rods to the top plate, detailed scheme of the assembly is shown in (Figure 2(b)).

After the bonding procedure several steps were followed, like the dimensional control, the ultrasound testing, the microscopic observations of the bonding plane as well as the tensile tests.

In order to calculate the permanent deformations, dimensional control was conducted after the diffusion bonding and from the variations before and after, the permanent deformations was extracted. The ultrasound testing was the first step for the qualification of the bonded joint by detecting possible defects. The representation of the data was a phased array C-Scan [15]. Whenever it was needed after the ultrasounds, the bonded stack was cut perpendicularly to the bonding plane and it was observed microscopically by doing crossing grain analysis. In case that the grains were crossing the interface (Figure 3(a)), the bonding was considered successful. Although, it happened that the ultrasound results did not

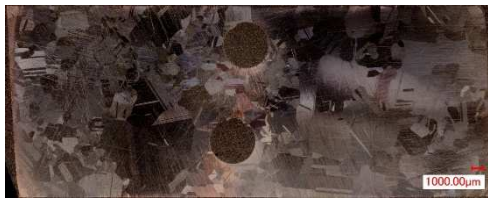
detect any defect and the microscopic observation did not show crossing grains or only a few small grain crossing (Figure 3(b)); in those cases it was not straight forward to judge the quality of the joint.



a) RF Disks tested under 0.1 MPa on the left and 0.28 MPa on the right, Ready to be placed into the furnace

b) Schematic representation of the configuration

Figure 2 : Picture of the tooling on the left and aschematic picture on the right.



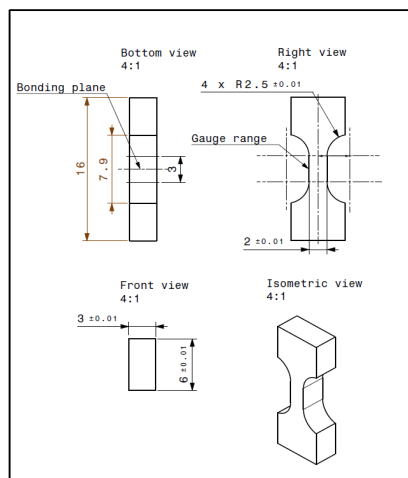
a) Microscopic Observation of a RF disk stack bonded without any applied load. The bonding plane is not recognized since big grains are crossing it.



b) Microscopic Observation of a simple disk stack bonded under 0.04 MPa, the bonding plane is easily recognized while only a small grain is crossing it on the Right Side.

Figure 3: Microscopic Observation of the interface of bonded samples.

In this respect, tensile tests were performed in order to quantify the ultimate tensile strength of the samples which have been bonded under different applied pressure values compared to raw material heat treated under the same heating cycle. One simple disk stack was chosen from each pressure case (0.04, 0.06, 0.1 and 0.28 MPa) and ten tensile samples were prepared by wire cutting. Figure 4 presents the size of the tensile samples as well as the experimental set up.



a) Drawing of the Tensile Samples



b) Experimental Set Up of the Tensile Tests

Figure 4: Tensile Tests Preparation and Conduction.

Varying the Applied Pressure

Focusing in the variable of the applied pressure bonding tests were conducted in two types of copper disks; simple disks without rf geometry, external diameter equal to $48 \text{ mm} \pm 10 \mu\text{m}$ and thickness of 8 mm and rf disks [16] with four damping waveguides (Figure 5), external diameter $80 \text{ mm} \pm 2 \mu\text{m}$ and thickness of 8.3 mm.

Both disks geometries had an ultra-high precision finishing using single crystal diamond tools. The dimensional control included measurements of the external diameter, the thickness and the flatness of each disk. Under the same pressure value, four configurations with simple disks and two configurations with rf disks were tested. The pressure values used are shown in Table 1.

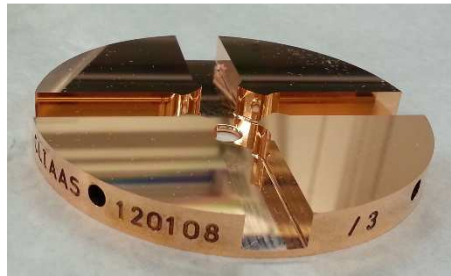


Figure 5: RF Disks with four Damping Waveguides.

After the bonding procedure the external diameter and the thickness were measured again using the aforementioned CMM machine. The ultrasound testing was applied in all disks and the microscopic observation in the majority of them. The tensile tests were performed only to the simple disks, since the extraction of the tensile samples was easier with this geometry.

Table 1: The Pressure Values Converted to Loads (kg).

Pressure (MPa)		0.04	0.06	0.1	0.28
Applied Load (kg)	Simple Disks	7.4	11.1	18.4	51.9
	rf Disks	16.3	24.5	40.8	114.2

VARYING THE INTERFACE FLATNESS

Investigating the parameter of the interface flatness, on the quality of the final bonded joint, only the flatness was measured during the dimensional control.

Table 2: Difference in the Flatness μm of the Interface.

Applied Pressure	Disk Stack	Bottom Plane	Top Plane	Min. diff. (μm)
No Pressure	#1	8.6	1.4	7.2
	#2	7.5	1.3	6.2
	#3	3.6	3.5	0.1
	#4	4.8	4.5	0.3
0.06 MPa	#5	14	5	9
	#6	13.1	4.1	9
	#7	3.4	2.6	0.8
	#8	2.4	2	0.4

Bonding tests had been performed with rf disks (Figure 5) without any additional pressure and under 0.06 MPa applied pressure. Two cases with high mismatching in the interface flatness and two with low mismatching had been bonded under each pressure value. In Table 2 the flatness of the faces in contact is given (in μm), as well as the absolute

difference between them. After the bonding procedure the bonded joint was checked by ultrasound test.

RESULTS

Varying the Applied Pressure

Permanent Deformations

Concerning the simple disks, the experimental results were compared with the theory predicted by the diffusion creep laws of Coble and Nabarro-Herring as well as the Finite Element Analysis model (FEA). On the other hand, the rf disks experimental results are compared only with the FEA model due to their complex design.

The simple disks geometry allowed the analytical approach with the Generalized Hooke's law for uni-axial compression. Considering that during the heating cycle the material deforms according to the two different mechanisms the surface diffusion and the volume diffusion, the deformation of the external diameter and the thickness are given from the Equations 3 and 4 respectively:

$$\Delta d = d \cdot \nu \cdot \left(\int_0^{0.7 T_m} \dot{\epsilon}_{co} T \cdot \Delta t + \int_{0.7 T_m}^{T_{max}} \dot{\epsilon}_{NH} T \cdot \Delta t \right) (3)$$

where d is the external diameter, ν is the Poisson's ratio which is taken equal to 0.31, $\dot{\epsilon}_{co}$ and $\dot{\epsilon}_{NH}$ is the strain rate, T is the time-varying temperature in a generic point of the heating cycle, T_m is the melting point of copper, T_{max} is the bonding temperature which is 1313 K and Δt is the time step used for the discrimination of the curve.

$$\Delta h = h \cdot \left(\int_0^{0.7 T_m} \dot{\epsilon}_{co} T \cdot \Delta t + \int_{0.7 T_m}^{T_{max}} \dot{\epsilon}_{NH} T \cdot \Delta t \right) (4)$$

Where h is the thickness of the disk.

Using Equations (3, 4) for the full heating cycle and the parameters given in Table 3, the theoretical results of the deformations in external diameter and thickness were calculated using Matlab for each pressure value.

The FEA model was built up in ANSYS Workbench. The properties of the Cu OFE had been implemented to the engineering data taking into account the temperature variation [17]. The creep property had been activated, adding the creep constant which was calculated from the two aforementioned creep laws. The surface diffusion was considered as dominant below this temperature value $0.7T_m$, where above this the volume diffusion. The creep parameter was calculated by the Equation (5) and the values were used as an input in the creep properties of the material.

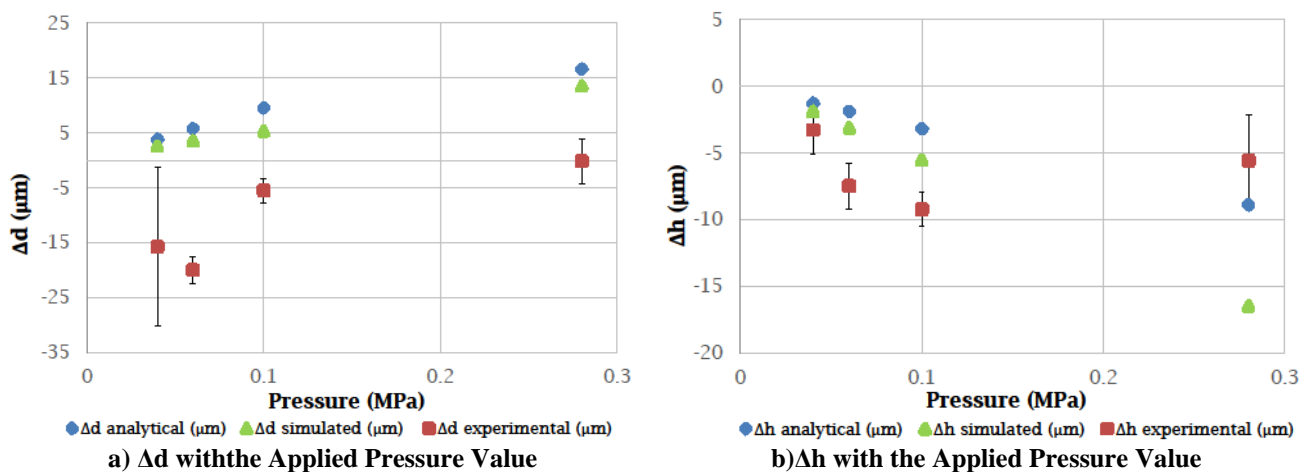
$$C_{Creep}(T) = \frac{A D \Omega}{d^n k T} \quad (5)$$

where A is the constant for Coble/ Nabarro-Herring, D is the diffusion coefficient for Coble/ Nabarro-Herring, Ω is the atomic volume, d is the grain size, n is equal to 3 for Coble and equal to 2 for Nabarro-Herring, k is the Boltzmann's constant and the T is the temperature.

Table 3: Parameters Used for Nabarro-Herring and Coble Diffusion Creep Law.

Description	Parameter	Value	Units
Gas constant	R	8.314	J/Kmol
Atomic volume	Ω	1.18×10^{-29}	m^3
Grain size	d	6.5×10^{-5}	m
Boltzmann constant	k	1.38×10^{-23}	J/K
Absolute temperature	T	Figure(1)	K
Nabarro-Herring constant	A_{NH}	12	
Coefficient for lattice boundary diffusion	D_1	$D_0 e^{-\frac{Q}{RT}}$	m^2/s
Pre-exponential	D_0	2×10^{-5}	m^2/s
Activation energy	Q	1.97×10^5	J/mol
Coble constant	A_{co}	$150/\pi$	
Coefficient for grain boundary diffusion	δD_{gb}	$D_b e^{-\frac{Q_b}{RT}}$	m^3/s
Pre-exponential	D_b	5×10^{-15}	m^3/s
Activation energy	Q_b	1.04×10^5	J/mol

The model was done in static structural analysis adding in the analysis settings 72 steps which they corresponded to the steps of the real heating cycle that was also implemented. Each step was equal to 600 sec. Only one quarter of the disk stack was examined in the model because the disk stack is symmetric in both lateral directions. Uni-axial compression was represented by an applied pressure on the top face of the disk stack and a zero displacement in the vertical direction of the bottom face. The contact between the disks was considered frictional. The comparison between the experimental results of the deformations, the theoretical and the simulated ones is presented in Figure 6 for the simple disks where Figure 7 presents the comparison between experimental and simulated results for the rf disks.

**Figure 6: Simple Disks Comparison of the Deformations which are given Experimentally, Analytically and from the FEA Simulations.**

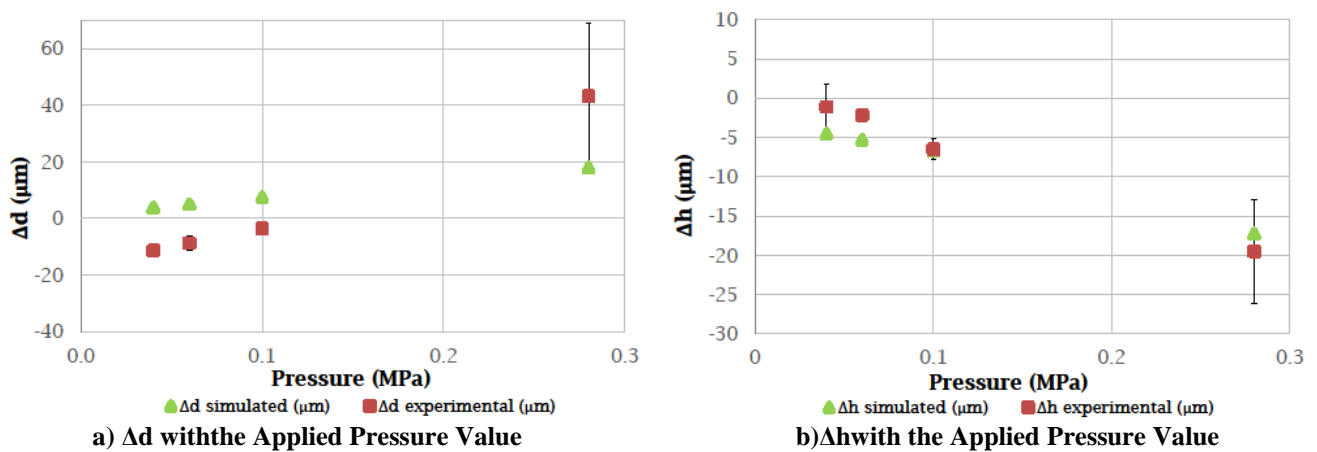


Figure 7: RFDisks Comparison of the Deformations which are given Experimentally and from the FEA Simulations.

Quality of the Bonded Joint

Ultrasound tests were performed in all the disk stacks after the dimensional control. The results showed no gap for all bonded stacks except from two. Those cases had been cut in order to perform microscopic observations. During these observations no gap was detected. Figure 8a presents the tensile results of the stack bonded with 0.04 MPa applied pressure. The value of the ultimate tensile strength for all the examined pressure cases is reasonably similar with significant standard deviations between samples of the same bonded stack, as it is shown in Figure 8b. This deviation between samples of the same bonded stack can be explained by considering the big grain size compared to the small size of the tensile samples.

Varying the Interface Flatness

The results of both examined pressure cases (having high and low mismatching in the interface flatness) were all very similar [15]. This drives to the conclusion that the interface flatness does not affect the final bonded joint for the values of flatness and pressure observed.

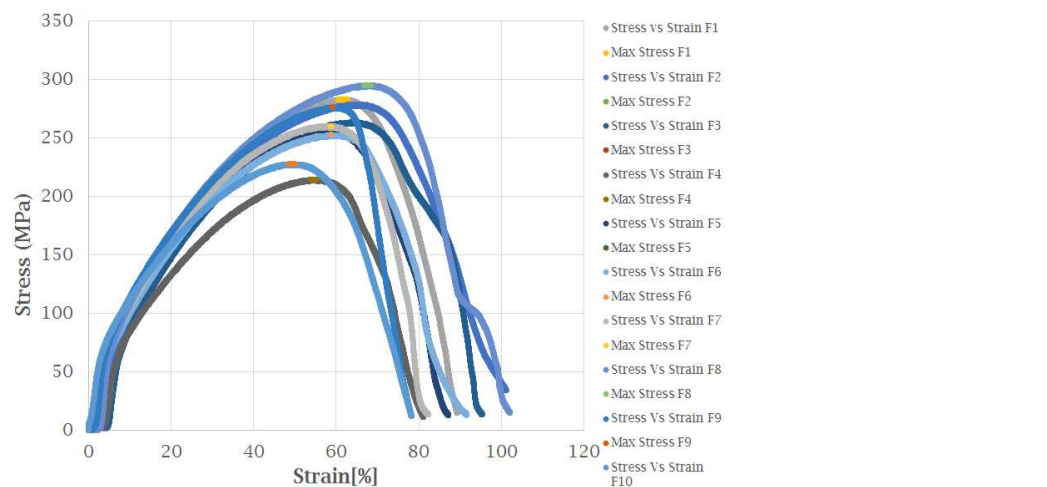


Figure 8: Results of a Stack, Bonded at 0.04 MPa.

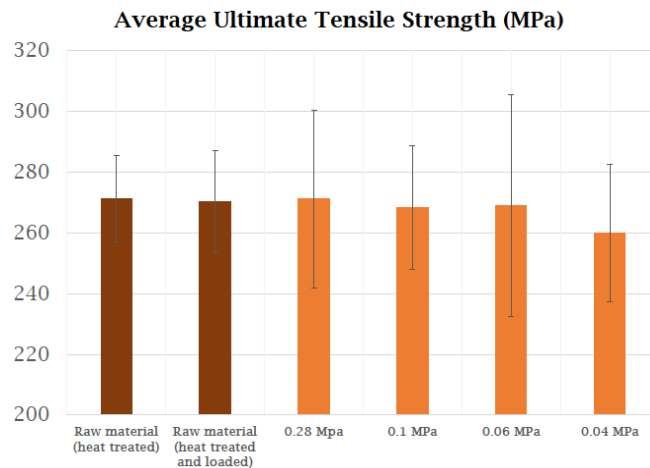


Figure 9: Average Ultimate Tensile Strength of six cases with their error bars.

DISCUSSIONS

Focusing in Figure 6 the diamonds present the results of the deformations calculated in an analytical way, while the simulated ones are presented with triangles. The squares give the averaged difference between measurements before and after the bonding process. It seems that the behavior of Δd is opposite to the Δh which is in accordance with the compression phenomenon. The comparison between analytical calculation and simulation shows better agreement for the deformation of the external diameter. Comparing both simulated and analytical results with the experimental data, it seems that they are not in perfect agreement. An unexpected shrinkage was observed on the external diameter which cannot be obtained analytically or by means of simulations. This shrinkage is converted through the volume variation to weight giving an average weight loss of 0.19 g. In addition to this, it is important to mention that during the heating cycle the average grain size (which is measured in room temperature) is increasing and this variation is not considered analytically or in the simulations. Concerning the results of the rf disks in Figure 7, the comparison between experimental and simulated results is in good agreement, especially for the Δh since a shrinkage in the external diameter is still present.

The experiments of the rf disks followed those of the simple disks and so the parameter of the weight was considered. Each rf disk of a stack was weighted before the bonding and was compared to the weight of the bonded disk stack. These results gave an average weight loss of 0.49 g with a standard deviation of 0.08 g. This value is not in agreement with the calculated weight loss from the volume variation, which is equal to 0.24 g. Normalizing those two values (0.19 g and 0.49 g) to the surfaces; an outcome of $1.97 \times 10^{-5} \text{ g/mm}^2$ and $2.08 \times 10^{-5} \text{ g/mm}^2$ is taken for the simple and RF disks, respectively. This verifies that the weight loss is present in all the experiments most probably because of a sublimation phenomenon that takes place at this high temperature. Calculating from Knudsen's equation [18] for vacuum the weight loss for the rf disks should be 1 g which is two times higher than the measured value. This difference can be attributed to the presence of H_2 which is reducing the sublimation. A shrinkage of 1 μm per cell had been reported in the past [19] after the diffusion bonding of a 1.3 m long x-band accelerating structure under vacuum and a temperature of 890 °C.

Concerning the bonded joint, it is worth to mention that the ultrasound testing is sufficient but not necessary way to detect any defect in the bonded joint. The results from both studies showed that neither the applied pressure nor the

interface flatness affect the bonded joint for the current heating cycle. Same results found from Molecular Dynamics simulations of copper atoms [20] where nano-voids on grain boundaries closed at the same bonding temperature without any additional pressure. The current temperature might overshadow all other parameters, since in previous bonding studies [21] at lower bonding temperature had shown dependence of the bonded joint quality on the interface flatness.

It is notable that the ultimate tensile strength of all pressure cases gives similar results although significant error bars appear. These bars indicate dissimilarity between the samples of each group. However, considering the size of the grain size after the heating cycle, compared to the size of the tensile samples this dissimilarity could not be avoided. The ultimate tensile strength of the heat treated raw material gives really close values with those of the bonded samples. This verifies the good bonded joint for all the pressure values.

CONCLUSIONS

Diffusion bonding tests have been conducted in OFE copper disks with simple and rf geometry varying the applied pressure and the interface flatness. The aim was to find a compromise between permanent deformations and bonded joint quality, so as to have as minor deformations as possible with a successful bonded joint. The theoretical approach which had been done analytically and with the FEA simulations; based on the surface diffusion at the low temperatures (Coble creep) and the volume diffusion at the higher (Nabarro-Herring diffusion creep) is quite representative to the reality. Although, shrinkage was observed in all cases in the external diameter and cannot be predicted neither from the analytical solution nor from the modeling. This shrinkage could be a result of sublimation phenomenon that takes place at these temperatures. However, a deeper analysis based on the sublimation rate under hydrogen in these elevated temperatures is highly encouraged for future studies. Concerning the bonded joint quality at the examined temperature, the results showed that it is not affected from the applied pressure or the interface flatness. This is verified further from the results of the tensile tests. The ultimate tensile strength of all the pressure cases is reasonably similar and has an average value of 267 MPa, which is very similar with the ultimate strength of the raw material. Additionally, it is worth to mention that the crossing grains in the interface of the two disks is a valid but not necessary criterion by which the successful bonded joint should be judged.

Concluding from these results, even a zero applied pressure combined with this heating cycle could result in an efficient bonding in terms of permanent deformations as well as bonded joint.

ACKNOWLEDGEMENTS

The authors gratefully acknowledge Dr. Fabrizio Rossi for the initial idea of this diffusion bonding tests and Dr. Nuria Catalan Lasheras for supporting the idea of the tensile tests. Mr. Serge Lebet is highly acknowledged for his valuable help in the conduction of the diffusion bonding tests.

REFERENCES

1. M. Aicheler et al. *A Multi-TeV linear collider based on CLIC technology: CLIC Conceptual Design Report*. CERN Geneva, Switzerland, 2012.
2. N. F. Kazakov. *Diffusion bonding of materials*. Elsevier, 2013.
3. Brian Derby and ER Wallach. *Theoretical model for diffusion bonding*. *Metal Science*, 16(1):49–56, 1982.

4. Hidetoshi Somekawa, Hiroyuki Hosokawa, Hiroyuki Watanabe, and Kenji Higashi. Diffusion bonding in superplastic magnesium alloys. *Materials Science and Engineering: A*, 339(1):328–333, 2003.
5. K Kitazono, A Kitajima, E Sato, J Matsushita, and K Kuribayashi. Solid-state diffusion bonding of closed-cell aluminum foams. *Materials Science and Engineering: A*, 327(2):128–132, 2002.
6. Jean-Paul Poirier. *Creep of crystals: high-temperature deformation processes in metals, ceramics and minerals*. Cambridge University Press, 1985.
7. RN Stevens. Grain boundary sliding and diffusion creep. *Surface Science*, 31:543–565, 1972.
8. Terence G Langdon. Identifying creep mechanisms at low stresses. *Materials Science and Engineering: A*, 283(1):266–273, 2000.
9. Terence G Langdon. Creep at low stresses: an evaluation of diffusion creep and harper-dorn creep as viable creep mechanisms. *Metallurgical and Materials Transactions A*, 33(2):249–259, 2002.
10. David M Owen and Terence G Langdon. Low stress creep behavior: An examination of nabarro herring and harper dorn creep. *Materials Science and Engineering: A*, 216(1):20–29, 1996.
11. Harold J Frost and Michael F Ashby. *Deformation mechanism maps: the plasticity and creep of metals and ceramics*. Pergamon press, 1982.
12. T Arkan, I Gonin, T Khabiboulline, D Finley, S Mishra, H Carter, N Solyak, E Borissov, C Boffo, and G Romanov. Fabrication of x-band accelerating structures at fermilab. Technical report, 2004.
13. Claude Sanz, Ahmed Cherif, Hélène Mainaud Durand, Paul Morantz, and Paul Shore. Characterisation and measurement to the sub-micron scale of a reference wire position. In *17th International Congress of Metrology*, page 13005. EDP Sciences, 2015.
14. A Degiovanni, S Doeber, W Farabolini, A Grudiev, J Kovermann, E Montesinos, G Riddone, I Syratcev, R Wegner, W Wuensch, et al. High-gradient test results from a clic prototype accelerating structure: Td26cc. In *WEPME015*, 2014.
15. Aline Piguiet. Clic: Ut of 8 stacks after diffusion bonding (td24 r0.5 sic), <https://edms.cern.ch/document/1459904/1>. Technical report, 2015.
16. A Solodko, D Gudkov, M Taborelli, S Atieh, A Samoshkin, G Riddone, and A Grudiev. Engineering design and fabrication of tapered damped x-band accelerating structures. Technical report, CERN Geneva, Switzerland, 2011.
17. Clair Upthegrove and Henry Lewis Burghoff. Elevated-temperature properties of coppers and copper-base alloys. *ASTM PAPERS*, 1956.
18. Herbert N Hersh. The vapor pressure of copper. *Journal of the American Chemical Society*, 75(7):1529–1531, 1953.
19. T Higo, H Sakai, Y Higashi, S Koike, T Takatomi, T Suzuki, K Takata, et al. Precise fabrication of 1.3 m-long x-band accelerating structure. In *Proc. 18th Int. Linear Accelerator Conf*, pages 96–07, 1996.
20. A Xydou, S Parviainen, M Aicheler, and F Djurabekova. Thermal stability of interface voids in cu at the grain boundaries with molecular dynamics simulations. *Journal of Physics D: Applied Physics*, under consideration, 2015.
21. Toshiro Kobayashi, Yasuo Higashi, Ritsuo Hashimoto, Tohru Takashina, Hideyuki Kanematsu, and Keiji Mizuta. Measuring flatness of ultrafine machined copper disk with laser interferometer and strength of diffusion bonding interface for high-energy accelerators. *Journal of the Japanese Society for Experimental Mechanics (JSEM)*, 13:s92–s95, 2013.

